Inorganic Chemistry
Article
pubs.acs.org/IC

Synthesis and Structural Characterization of Ruthenium Carbonyl Cluster Complexes Containing Platinum with a Bulky N-Heterocyclic Carbene Ligand

Sumit Saha and Burjor Captain*

Department of Chemistry, University of Miami, Coral Gables, Florida 33124, United States

Supporting Information

ABSTRACT: The reaction of $Ru_3(CO)_{12}$ with $Pt(IMes)_2$ in benzene solvent at room temperature afforded the monoplatinum−triruthenium cluster complex $Ru_3Pt(IMes)_2(CO)_{11}$, **1**, in 21% yield and the trigonal bipyramidal cluster complex $Ru_3Pt_2(IMes)_2(CO)_{12}$, **2**, in 26% yield. The reaction of $Ru(CO)_5$ with $Pt(IMes)_2$ in benzene solvent at 0 °C yielded two trinuclear cluster complexes, the monoplatinum−diruthenium $Ru_2Pt(IMes)(CO)_9$, **3**, and the monoruthenium−diplatinum cluster complex $RuPt_2(IMes)_2(CO)_6$, **4**. The reaction of **2** with hydrogen at 80 °C afforded the tetrahydrido−tetraruthenium complex $Ru_4(IMes)(CO)_{11}(\mu\text{-H})_4$, **5**, and the dihydrido−diruthenium−diplatinum complex $Ru_2Pt_2(IMes)_2(CO)_8(\mu\text{-H})_2$, **6**. All six compounds were structurally characterized by single-crystal X-ray diffraction analyses.

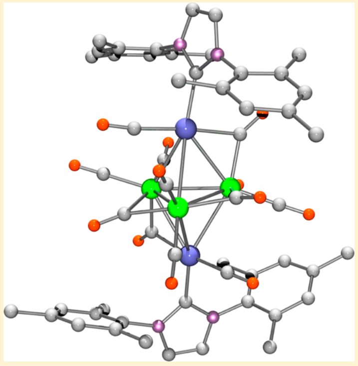

INTRODUCTION

In 1994, Arduengo synthesized and characterized low-coordinate NHC complexes of nickel(0) and platinum(0).[1] Ever since this report, the synthesis of N-heterocyclic carbenes (NHCs), as well as the use of NHCs as ligands in coordination chemistry, has attracted significant attention.[2] With the use of novel NHC−metal complexes, many important reactions, such as olefin metathesis,[3] Pd-catalyzed cross-coupling reactions,[4] and hydrogenation reactions,[5] have shown noticeable improvements. The strong electron-donating properties of NHCs often give their metal complexes increased stability.[6] As a result of their electronic properties, NHCs provide a versatile alternative to phosphine ligands. They also provide an equally variable steric environment, which is quite different from that of phosphines. Thus, substitution of a phosphine ligand with an NHC can lead to a dramatic increase in catalytic activity and stability.[6,7] The synthesis of novel NHC−Pt(0) complexes has been previously reported, and their efficiency in the hydrosilylation of a broad range of alkenes was demonstrated.[8] NHC−$Pt(alkene)_2$ complexes were also shown to be used as hydrosilylation catalysts.[9]

While there has been considerable work done with mono nuclear−NHC complexes, metal clusters with NHC have been less than studied. Mixed-metal cluster complexes have been shown to be good precursors for the preparation of supported bimetallic nanoparticles.[10] It has been shown that certain bimetallic catalysts have both higher activity and better product selectivity than their monometallic counterparts.[11] Supported platinum−ruthenium clusters have been shown to exhibit high activity for catalytic hydrogenation reactions when immobilized on mesoporous silica.[12,13] The use of NHCs in metal cluster chemistry is still relatively limited. To the best of our knowledge, bimetallic Ru−Pt−NHC cluster complexes have not yet been investigated.

Thus, we have now studied the reaction of $Ru_3(CO)_{12}$ and $Ru(CO)_5$ with 2,2′-bis(1,3-dimesitylimidazol-2-ylidene)-platinum(0), $Pt(IMes)_2$, to yield four new Ru−Pt−NHC cluster complexes. Furthermore, we also investigated the reaction of hydrogen with some of these complexes. The synthesis and structural characterization of these new bimetallic N-heterocyclic carbene compounds are presented in this article.

EXPERIMENTAL SECTION

General Data. Unless indicated otherwise, all reactions were performed under an atmosphere of argon. Reagent grade solvents were dried by the standard procedures and were freshly distilled prior to use. Infrared spectra were recorded on a Nicolet 380 FT-IR spectrophotometer. ^{1}H NMR were recorded on a Bruker 400 and 500 spectrometer operating at 399.993 and 500.06 MHz, respectively. Electrospray mass spectrometric measurements were obtained on a Bruker microTOF-Q II at the University of Miami, Coral Gables, FL, and mass spectrometric measurements performed by direct-exposure probe using electron impact ionization (EI) were made on a VG 70S instrument at the University of South Carolina, Columbia, SC. $Ru_3(CO)_{12}$ was purchased from Alfa Aesar and was used without further purification. 2,2′-bis(1,3-dimesitylimidazol-2-ylidene)-platinum(0), $Pt(IMes)_2$, was prepared according to the previously published procedure,[1] and stored and handled in a drybox. Product separations were performed by TLC in air on Analtech silica gel GF 250 or 500 μm glass plates.

Received: November 12, 2013
Published: January 3, 2014

Reaction of $Ru_3(CO)_{12}$ with $Pt(IMes)_2$. A 20 mg (0.03 mmol) amount of $Ru_3(CO)_{12}$ and 84 mg (0.10 mmol) amount of $Pt(IMes)_2$ were dissolved in 20 mL of benzene in a 50 mL Schlenk tube in a drybox. The solution was then stirred at room temperature for 5 min at which time IR showed complete consumption of the starting $Ru_3(CO)_{12}$. The solvent was removed in vacuo, and the product was separated by TLC on silica gel by using 2:1 hexane/methylene chloride solvent mixture to yield 9.2 mg (21%) of purple $Ru_3Pt(IMes)_2(CO)_{11}$, **1**, 13.4 mg (26%) of brown $Ru_3Pt_2(IMes)_2(CO)_{12}$, **2**, and 3.5 mg (12%) of yellow $Ru_2Pt(IMes)(CO)_9$, **3**. Spectral data for **1**, IR ν_{CO} (cm^{-1} in hexane): 2076 (w), 2023 (m), 2001 (s), 1980 (w), 1957 (m), 1844 (m), 1795 (m). ^1H NMR (CD_2Cl_2 in ppm, 400 MHz): δ = 7.14 (s, 2H, NCH), 7.11 (s, 4H, *m*-H), 6.94 (s, 4H, *m*-H), 6.78 (s, 2H, NCH), 2.46 (s, 6H, *p*-CH_3), 2.31 (s, 6H, *p*-CH_3), 2.01 (s, 12H, *o*-CH_3), 1.98 (s, 12H, *o*-CH_3). ESI: *m*/*z* 1417 (M^+). The isotope distribution pattern is consistent with the presence of one platinum atom and three ruthenium atoms. Spectral data for **2**, IR ν_{CO} (cm^{-1} in methylene chloride): 2051 (w), 2012 (s), 1988 (m), 1963 (w), 1943 (m), 1869 (w), 1815 (m), 1743 (m). ^1H NMR (CD_2Cl_2 in ppm, 400 MHz): δ = 7.09 (s, 4H, NCH), 6.87 (s, 8H, *m*-H), 2.28 (s, 12H, *p*-CH_3), 1.91 (s, 24H, *o*-CH_3). ESI: *m*/*z* 1661 (M^+ + Na). The isotope distribution pattern is consistent with the presence of two platinum atoms and three ruthenium atoms. Spectral data for **3**, IR ν_{CO} (cm^{-1} in methylene chloride): 2102 (w), 2084 (w), 2066 (m), 2025 (s), 1975 (m), 1836 (m), 1816 (m). ^1H NMR (C_6D_6 in ppm, 400 MHz): δ = 6.59 (s, 4H, *m*-H), 6.26 (s, 2H, NCH), 2.05 (s, 12H, *o*-CH_3), 1.94 (s, 6H, *p*-CH_3). ESI: *m*/*z* 977 (M^+ + Na). The isotope distribution pattern is consistent with the presence of one platinum atom and two ruthenium atoms.

Reaction of $Ru(CO)_5$ with $Pt(IMes)_2$. A solution of $Ru(CO)_5$ was prepared and used in situ as follows.[14] A 40 mg (0.06 mmol) amount of $Ru_3(CO)_{12}$ was dissolved in 120 mL of hexane in a 250 mL three-neck flask. The solution was placed in an ice-bath and was irradiated using a high-pressure mercury 1000 W UV lamp (American Ultraviolet Co.) at the 125 W per inch setting while CO gas was bubbled through it for 15 min. During this time, the orange colored solution turned colorless, and IR showed the formation of $Ru(CO)_5$. The reaction flask was then evacuated and filled with argon several times to remove the excess CO gas. A 150 mg (0.19 mmol) amount of $Pt(IMes)_2$ was dissolved in 20 mL of benzene in a 50 mL Schlenk tube in a drybox and then added to the $Ru(CO)_5$ solution at 0 °C via a cannula. The solution was then allowed to warm to room temperature and stirred for 10 min at which time IR showed complete consumption of the starting $Ru(CO)_5$. The solvent was removed in vacuo, and the product was separated by TLC on silica gel by using hexane solvent to yield 8.1 mg (15%) of yellow $Ru_2Pt(IMes)(CO)_9$, **3**, and 14.0 mg (21%) of orange $RuPt_2(IMes)_2(CO)_6$, **4**. Spectral data for **4**, IR ν_{CO} (cm^{-1} in hexane): 2071 (m), 1999 (vs), 1970 (vs), 1808 (vs), 1781 (s). ^1H NMR (C_6D_6 in ppm, 400 MHz): δ = 6.65 (s, 8H, *m*-H), 6.40 (s, 4H, NCH), 2.16 (s, 24H, *o*-CH_3), 2.08 (s, 12H, *p*-CH_3). ESI: *m*/*z* 1291 (M^+ + Na). The isotope distribution pattern is consistent with the presence of two platinum atoms and one ruthenium atom.

Reaction of $Ru_3Pt_2(IMes)_2(CO)_{12}$, 2, with H_2. A 20 mg (0.03 mmol) amount of $Ru_3Pt_2(IMes)_2(CO)_{12}$, **2**, was dissolved in benzene in a 50 mL three-neck round-bottom flask equipped with a reflux condenser, stir bar, and gas inlet. The solution was then purged with hydrogen (1 atm) for 15 min at 80 °C at which time IR showed complete consumption of the starting material, **2**. The solvent was removed in vacuo, and the product was separated by TLC on silica gel by using 1:1 hexane/methylene chloride solvent mixture to yield 1.5 mg (12%) of yellow $Ru_4(IMes)(CO)_{11}(\mu\text{-}H)_4$, **5**, and 6.2 mg (36%) of orange $Ru_2Pt_2(IMes)_2(CO)_8(\mu\text{-}H)_2$, **6**. Spectral data for **5**, IR ν_{CO} (cm^{-1} in hexane): 2083 (m), 2061 (w), 2048 (vs), 2028 (s), 2002 (m), 1986 (m), 1967 (w). ^1H NMR (C_6D_6 in ppm): δ = 6.78 (s, 4H, m-H), 5.87 (s, 2H, NCH), 2.09 (s, 6H, *p*-CH_3), 1.92 (s, 12H, *o*-CH_3), −17.67 (s, broad, 4H, hydride). EI/MS: *m*/*z* 1022 (M^+), 994 (M^+ − CO). The isotope distribution pattern is consistent with the presence of four ruthenium atoms. Spectral data for **6**, IR ν_{CO} (cm^{-1} in hexane): 2046 (m), 2013 (vs), 2002 (w), 1988 (w), 1972 (s), 1950 (w), 1936 (m). ^1H NMR (CD_2Cl_2 in ppm, 500 MHz): δ = 7.00 (s, 4H, NCH), 6.91 (s, 4H, *m*-H), 6.84 (s, 4H, *m*-H), 2.27 (s, 12H, *p*-CH_3), 2.01 (s, 12H, *o*-CH_3), 1.83 (s, 12H, *o*-CH_3), −9.89 (s, 2H, $^1J_{Pt-H}$ = 560 Hz, $^2J_{Pt-H}$ = 40 Hz, hydride). ESI: *m*/*z* 1428 (M^+). The isotope distribution pattern is consistent with the presence of two platinum atoms and two ruthenium atoms.

Reaction of $Ru_2Pt(IMes)(CO)_9$, 3, with $Pt(IMes)_2$. A 20 mg (0.02 mmol) amount of $Ru_2Pt(IMes)(CO)_9$, **3**, was dissolved in 20 mL of benzene in a 50 mL three-neck round-bottom flask equipped with a reflux condenser. A 17 mg (0.02 mmol) amount of $Pt(IMes)_2$ was dissolved in 10 mL of benzene in a 25 mL Schlenk tube in a drybox and added to the solution of compound **3** through cannula. The solution was then refluxed at 80 °C for 60 min at which time IR showed complete consumption of the starting material, **3**. The solvent was removed in vacuo, and the product was separated by TLC on silica gel by using 2:1 hexane/methylene chloride solvent mixture to yield 10.0 mg (38%) of orange $RuPt_2(IMes)_2(CO)_6$, **4**, and 2.0 mg (6%) of brown $Ru_3Pt_2(IMes)_2(CO)_{12}$, **2**.

Note: The same result was obtained when trimethyl amine *N*-oxide, Me_3NO, was added to a benzene solution of $Ru_2Pt(IMes)(CO)_9$, **3**, and $Pt(IMes)_2$.

Crystallographic Analysis. Single crystals of **1**, **3**, and **6** suitable for diffraction analysis were all grown by slow evaporation of solvent from solutions in methylene chloride/hexane solvent mixture at −25 °C. Single crystals of compounds **2** and **5** suitable for diffraction analysis were grown by slow evaporation of solvent from solutions in methylene chloride/toluene/octane and ether solvent mixture, respectively, at −25 °C. Single crystals of compound **4** suitable for diffraction analysis were grown by slow evaporation of solvent from solutions in benzene/octane solvent mixture at 6 °C. The data crystals for **1**, **3**, **4**, and **5** were glued onto the end of a thin glass fiber. The data crystals for **2** and **6** were mounted onto the end of a thin glass fiber using Paratone-N. X-ray intensity data were measured by using a Bruker SMART APEX2 CCD-based diffractometer using Mo Kα radiation (λ = 0.71073 Å).[15] The raw data frames were integrated with the SAINT+ program by using a narrow-frame integration algorithm.[15] Corrections for Lorentz and polarization effects were also applied with SAINT+. An empirical absorption correction based on the multiple measurement of equivalent reflections was applied using the program SADABS. All structures were solved by a combination of direct methods and difference Fourier syntheses, and refined by full-matrix least-squares on F^2, by using the SHELXTL software package.[16] All non-hydrogen atoms were refined with anisotropic displacement parameters. Hydrogen atoms were placed in geometrically idealized positions and included as standard riding atoms during the least-squares refinements. Crystal data, data collection parameters, and results of the analyses are listed in Tables 1, 2, and 3.

Compounds **1**, **2**, **4**, and **6** crystallized in the monoclinic crystal system. For compounds **1** and **4**, the systematic absences in the intensity data were consistent with the unique space group $P2_1/c$. For compound **1**, with Z = 8 there are two formula equivalents of the complex in the asymmetric crystal unit. The *R* value is high because of poor data quality and the large number of parameters. Low temperature data set at 100 K also gave results with high *R* values. Several attempts were made to obtain “better” quality crystals from various different solvents; however, only thin tiny plates were obtained, or large blocks of crystals that were severely twinned. Other characterization data (provided above) are consistent with the solved structure. For compound **4**, the Ru atom is disordered over two closely spaced orientations and was refined in the ratio 88:12. Likewise, the three CO groups on Ru are disordered and were modeled in a 88:12 ratio. The minor disorder component of the CO ligands was refined with isotropic thermal parameters. For compound **2**, the systematic absences in the intensity data were consistent with the unique space group $P2_1/n$. For compound **2**, a chemically reasonable starting solution provided good positions for all Pt, Ru, and most O, N, and C atoms, but yielded negative thermal parameters for some of the nonheavy metal atoms, high *R* factors (R1 ~25%), some large electron density peaks, which are chemically unreasonable, a systematic pattern of $F_{obs} \gg F_{calc}$, and all attempts to solve the

Table 1. Crystallographic Data for Compounds $Ru_3Pt(IMes)_2(CO)_{11}$, **1**, and $Ru_3Pt_2(IMes)_2(CO)_{12}$, **2**

	1	2
empirical formula	$PtRu_3C_{53}H_{48}N_4O_{11}$	$Pt_2Ru_3C_{54}H_{48}N_4O_{12}$
formula weight	1415.25	1638.35
crystal system	monoclinic	monoclinic
lattice parameters		
a (Å)	18.081(1)	16.4415(9)
b (Å)	41.675(2)	15.8001(9)
c (Å)	16.910 (1)	20.6466(12)
α (deg)	90	90
β (deg)	90.162 (1)	90.086 (1)
γ (deg)	90	90
V (Å^3)	12 742.1(13)	5363.5(5)
space group	$P2_1/c$ (No. 14)	$P2_1/n$ (No. 14)
Z value	8	4
ρ_{calc} (g/cm^3)	1.475	2.029
μ(Mo Kα) (mm^{-1})	2.938	6.088
temp (K)	296	100
$2\Theta_{max}$ (deg)	50.00	55.00
no. obs. ($I > 2\sigma(I)$)	12 533	11 033
no. parameters	1278	689
GOF	1.113	1.110
max shift in cycle	0.002	0.002
residuals:^{a} R1; wR2	0.1060; 0.2205	0.0485; 0.1155
absorption correction	multiscan	multiscan
max/min	0.6199/0.4727	0.8879/0.2805
largest peak in final diff. map (e$^-$/Å^3)	2.009	3.970

$^a R = \sum_{hkl}(||F_{obs}| - |F_{calc}||)/\sum_{hkl}|F_{obs}|$; $R_w = [\sum_{hkl}w(|F_{obs}| - |F_{calc}|)^2/\sum_{hkl}wF_{obs}^2]^{1/2}$, $w = 1/\sigma^2(F_{obs})$; GOF = $[\sum_{hkl}w(|F_{obs}| - |F_{calc}|)^2/(n_{data} - n_{vari})]^{1/2}$.

Table 2. Crystallographic Data for Compounds $Ru_2Pt(IMes)(CO)_9$, **3**, and $RuPt_2(IMes)_2(CO)_6$, **4**

	3	4
empirical formula	$PtRu_2C_{30}H_{20}N_2O_9$	$Pt_2RuC_{48}H_{48}N_4O_6$
formula weight	949.71	1268.15
crystal system	triclinic	monoclinic
lattice parameters		
a (Å)	9.0916(3)	22.2711(9)
b (Å)	10.8002(4)	10.6747(4)
c (Å)	18.0566(7)	22.7224(9)
α (deg)	81.060 (1)	90
β (deg)	80.374 (1)	117.779 (1)
γ (deg)	72.777 (1)	90
V (Å^3)	1659.06(10)	4779.4(3)
space group	$P\bar{1}$ (No. 2)	$P2_1/c$ (No. 14)
Z value	2	4
ρ_{calc} (g/cm^3)	1.901	1.762
μ(Mo Kα) (mm^{-1})	5.156	6.201
temp (K)	296	296
$2\Theta_{max}$ (deg)	56.00	56.00
no. obs. ($I > 2\sigma(I)$)	7404	9690
no. parameters	397	593
GOF	1.081	1.024
max shift in cycle	0.004	0.001
residuals:^{a} R1; wR2	0.0231; 0.0573	0.0248; 0.0593
absorption correction	multiscan	multiscan
max/min	0.7461/0.5443	0.8860/0.3702
largest peak in final diff. map (e$^-$/Å^3)	0.735	1.597

$^a R = \sum_{hkl}(||F_{obs}| - |F_{calc}||)/\sum_{hkl}|F_{obs}|$; $R_w = [\sum_{hkl}w(|F_{obs}| - |F_{calc}|)^2/\sum_{hkl}wF_{obs}^2]^{1/2}$, $w = 1/\sigma^2(F_{obs})$; GOF = $[\sum_{hkl}w(|F_{obs}| - |F_{calc}|)^2/(n_{data} - n_{vari})]^{1/2}$.

structure in the orthorhombic crystal system were unsuccessful considering the β angle was very close to 90°, which is indicative of some form of crystal twinning. The appropriate twin law common for a monoclinic system with the beta angle close to 90° is a 2-fold rotation about the [100] direction. The corresponding twin law is, by rows, $\{100/0\bar{1}0/00\bar{1}\}$. This twin law was implemented in the final refinement stages to give low R factors (R1 = 4.85%) and good thermal parameters. The highest peak in the final difference Fourier map was 3.970 e$^-$/Å^3, located 0.99 Å from atom Pt(1). The final refined batch scale factor indicated the crystal to be composed of two twin domains of percentage 0.5209(4)/0.4791(4). For compound **6**, the systematic absences in the intensity data were consistent with the space groups $C2$, $C2/m$, or Cm. The structure could only be solved in the space group $C2$. Hydrides in this structure were not located crystallographically, but their presence was confirmed by ^{1}H NMR. Two molecules of CH_2Cl_2 from the crystallization solvent cocrystallized with the complex and were included in the crystal analysis.

Compounds **3** and **5** crystallized in the triclinic crystal system. The space group $P\bar{1}$ was chosen for both and confirmed by the successful solution and refinement of the structure. The hydride ligands in **5** were located and refined successfully with isotropic thermal parameters. Atoms H1 and H4 were refined with a fixed isotropic thermal parameter.

■ RESULTS AND DISCUSSION

The reaction of triruthenium dodecacarbonyl, $Ru_3(CO)_{12}$, with 2,2′-bis(1,3-dimesitylimidazol-2-ylidene)platinum(0), Pt(IMes)$_2$, in benzene solvent at room temperature afforded two new bimetallic cluster complexes, the monoplatinum−triruthenium cluster complex $Ru_3Pt(IMes)_2(CO)_{11}$, **1**, in 21% yield and the diplatinum−triruthenium cluster complex $Ru_3Pt_2(IMes)_2(CO)_{12}$, **2**, in 26% yield. Both compounds **1** and **2** were structurally characterized by a combination of IR, ^{1}H NMR, mass spectrometry, and single-crystal X-ray diffraction analyses. An ORTEP depicting the molecular structure of **1** is shown in Figure 1.

Compound **1** consists of a square plane with three ruthenium atoms and one platinum atom, and can be viewed as two triangles that share an edge formed by a Ru−Ru single bond, Ru1−Ru2 = 2.892(3) Å. The Pt(IMes) group is an edge bridging on the Ru_3 triangle. There is also an IMes group that is coordinated to atom Ru3 opposite the Pt atom. There are two bridging carbonyl groups that bridge the ruthenium− platinum bonds. The IMes group on Ru3 lies perpendicularly to the Ru_3 triangular plane. Cabeza et al. have previously reported the reaction of $Ru_3(CO)_{12}$ with *N*,*N*′-dimesitylimidazol-2-ylidene (Mes$_2$Im), which afforded the trinuclear NHC substituted complex [Ru_3(Mes$_2$Im)(CO)$_{11}$], where one ruthenium atom is bonded with the IMes group.[17]

The structure of complex **2** in the solid state is given in Figure 2. Compound **2** has a trigonal bipyramidal geometry of three ruthenium atoms and two platinum atoms. The Ru atoms occupy the equatorial plane, while the Pt atoms occupy the apical positions of the trigonal bipyramid. With no loss of CO ligands, compound **2** can be viewed as an adduct of $Ru_3(CO)_{12}$, where two Pt(IMes) groups cap the Ru_3 triangle. The two carbonyl ligands coordinated to each of the Pt atoms are edge bridging and slightly semibridging in nature, Pt1−C10−O10 = 172.6(10)° and Pt2−C20−O20 = 172.9(12)°. Adams et al. have prepared the pentanuclear platinum−osmium compound $Pt_2Os_3(CO)_{10}(P^tBu_3)_2$,[18] which has a structure similar to

Table 3. Crystallographic Data for Compounds $Ru_4(IMes)(CO)_{11}(\mu\text{-}H)_4$, **5**, and $Ru_2Pt_2(IMes)_2(CO)_8(\mu\text{-}H)_2$, **6**

	5	6
empirical formula	$Ru_4C_{32}H_{28}N_2O_{11}$	$Pt_2Ru_2C_{50}H_{48}N_4O_8\cdot 2CH_2Cl_2$
formula weight	1020.84	1595.10
brystal system	triclinic	monoclinic
lattice parameters		
a (Å)	11.1505(5)	18.1662(9)
b (Å)	11.3048(5)	17.0073(9)
c (Å)	15.8466(7)	12.9425(7)
α (deg)	108.061 (1)	90
β (deg)	99.189 (1)	130.851(1)
γ (deg)	94.688 (1)	90
V (Å^3)	1856.31(14)	3024.7(3)
space group	$P\bar{1}$ (No. 2)	$C2$ (No. 5)
Z value	2	2
ρ_{calc} (g/cm^3)	1.826	1.751
μ(Mo Kα) (mm^{-1})	1.653	5.327
temp (K)	296	100
$2\Theta_{max}$ (deg)	60.00	62.00
no. obs. ($I > 2\sigma(I)$)	7738	8914
no. parameters	460	331
GOF	1.000	1.056
max shift in cycle	0.002	0.002
residuals:[a] R1; wR2	0.0324; 0.0623	0.0309; 0.0939
absorption correction	multiscan	multiscan
max/min	0.7461/0.6543	0.7465/0.4030
largest peak in final diff. map (e$^-$/Å^3)	0.509	4.561

[a] $R = \sum_{hkl}(||F_{obs}| - |F_{calc}||)/\sum_{hkl}|F_{obs}|$; $R_w = [\sum_{hkl}w(|F_{obs}| - |F_{calc}|)^2/\sum_{hkl}wF_{obs}^2]^{1/2}$, $w = 1/\sigma^2(F_{obs})$; GOF $= [\sum_{hkl}w(|F_{obs}| - |F_{calc}|)^2/(n_{data} - n_{vari})]^{1/2}$.

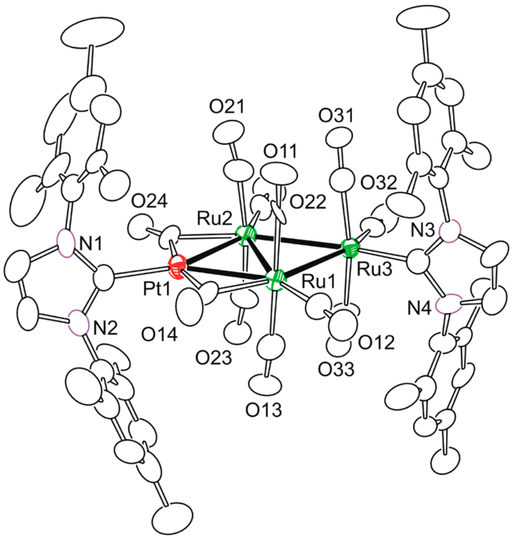

Figure 1. An ORTEP showing the molecular structure of $Ru_3Pt(IMes)_2(CO)_{11}$, **1**, at 30% thermal ellipsoid probability. Selected interatomic distances (Å) and angles (deg) are as follows: Pt(1)−Ru(1) = 2.699(2), Pt(1)−Ru(2) = 2.691(2), Ru(1)−Ru(2) = 2.892(3), Ru(1)−Ru(3) = 2.890(3), Ru(2)−Ru(3) = 2.915(3), Ru(2)−Pt(1)−Ru(1) = 64.90(6), Pt(1)−Ru(1)−Ru(3) = 117.94(8), Pt(1)−Ru(2)−Ru(1) = 57.69(6), Ru(1)−Ru(3)−Ru(2) = 59.76(6).

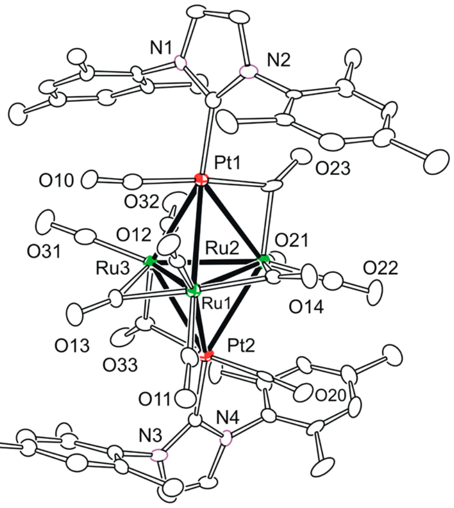

Figure 2. An ORTEP showing the molecular structure of $Ru_3Pt_2(IMes)_2(CO)_{12}$, **2**, at 50% thermal ellipsoid probability. Selected interatomic distances (Å) and angles (deg) are as follows: Pt(1)−Ru(2) = 2.833(1), Pt(1)−Ru(1) = 2.938(1), Pt(1)−Ru(3) = 2.939(1), Pt(2)−Ru(3) = 2.810(1), Pt(2)−Ru(2) = 2.912(1), Pt(2)−Ru(1) = 2.995(1), Ru(2)−Ru(1)−Ru(3) = 65.33(3), Ru(1)−Pt(1)−Ru(3) = 55.62(3), Ru(3)−Pt(2)−Ru(1) = 56.26(3).

compound **2** but contains two less CO ligands. In the previously reported reactions of $Ru_3(CO)_{12}$ with $Pd(P^tBu_3)_2$,[19] and $Os_3(CO)_{12}$ with $Pd(P^tBu_3)_2$[20] or $Pt(P^tBu_3)_2$,[21] similar products were obtained where the $Pd(P^tBu_3)$ or $Pt(P^tBu_3)$ groups add across the metal−metal bonds in these reactions to form edge bridging raft-like complexes, as shown in Figure 3.

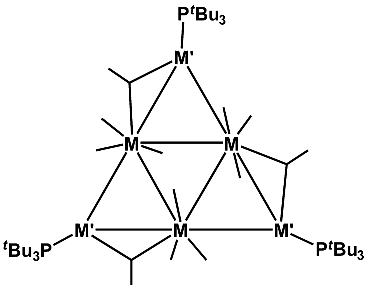

Figure 3. Structure of $M(CO)_{12}[M'(P^tBu_3)]_3$ where M = Ru and M′ = Pd; M = Os and M′ = Pd or Pt.

It is interesting to note that in our reaction only two Pt(IMes) groups were able to add to $Ru_3(CO)_{12}$ to give **2**, indicating the steric differences between the IMes and P^tBu_3. The complex $Pt_2Os_3(CO)_{10}(P^tBu_3)_2$ instead was obtained from $Os_3(CO)_{10}(NCMe)_2$ and $Pt(P^tBu_3)_2$.[18]

Another product $Ru_2Pt(IMes)(CO)_9$, **3**, was also obtained as a result of this reaction, but in lower yields, due to fragmentation of the $Ru_3(CO)_{12}$ reagent. Thus, one could obtain this complex directly from $Ru_2(CO)_9$ and $Pt(IMes)_2$. However, because of the high instability of $Ru_2(CO)_9$, it was not possible to perform this reaction.[22] Instead, we carried out the reaction of $Ru(CO)_5$ with $Pt(IMes)_2$. $Ru(CO)_5$ reacts with $Pt(IMes)_2$ in benzene solvent at 0 °C to afford the bimetallic trinuclear cluster complexes, $Ru_2Pt(IMes)(CO)_9$, **3** (15% yield), and $RuPt_2(IMes)_2(CO)_6$, **4** (21% yield). Both compounds **3** and **4** were also characterized crystallographically.

As shown in Figure 4, compound **3** contains a triangle of three metal atoms of which two are ruthenium atoms and one is a platinum atom. There are three bridging carbonyl ligands that bridge each of the Pt−Ru bonds and a Ru−Ru bond. With nine CO ligands, this compound can be viewed as a monoplatinum adduct of $Ru_2(CO)_9$. As expected, the Ru−Ru bond distance (2.8658 Å) is very close to the Ru1−Ru2 bond length in **1** (2.892(3) Å), due to similar donation of electrons from the Ru1−Ru2 bond to the platinum atom. Complex **2** is similar in structure to $PtRu_2(CO)_9(PBu^t{}_3)$,[23] which was obtained from the reaction of $Ru(CO)_5$ with $Pt(P^tBu_3)_2$.

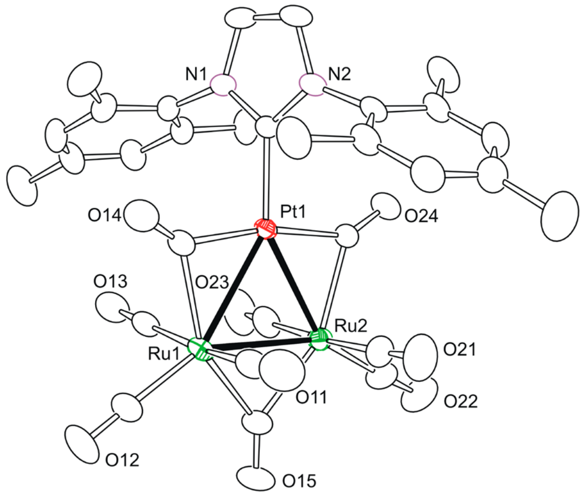

Figure 4. An ORTEP showing the molecular structure of $Ru_2Pt(IMes)(CO)_9$, **3**, at 30% thermal ellipsoid probability. Selected interatomic distances (Å) and angles (deg) are as follows: Pt(1)−Ru(2) = 2.7161(3), Pt(1)−Ru(1) = 2.7241(3), Ru(1)−Ru(2) = 2.8658(4), Ru(2)−Pt(1)−Ru(1) = 63.576(8), Pt(1)−Ru(1)−Ru(2) = 58.077(7), Pt(1)−Ru(2)−Ru(1) = 58.347(8).

Compound **4** is another trinuclear cluster complex that was furnished in this reaction but contains two platinum atoms and one ruthenium atom. Its structure in the solid state (see Figure 5) consists of a $RuPt_2$ triangle with the IMes groups located on the platinum atoms.

Interestingly, the ruthenium atom just as in **3** has five carbonyl ligands, two of which bridge to the neighboring Pt atoms and the other three carbonyl ligands are terminally coordinated. The sixth carbonyl ligand bridges the two platinum atoms, Pt1 and Pt2. The Pt−Pt bond distance (2.6477 Å) is shorter than the Ru−Pt bond distances (av 2.7091 Å).

A comprehensive study of the chemistry of bimetallic cluster complexes containing the bulky $Pd(P^tBu_3)$ or $Pt(P^tBu_3)$ groups has shown interesting reactivity, especially with hydrogen gas.[24] Thus, we investigated the reaction of compound **2** with H_2, which afforded the tetrahydrido−tetraruthenium complex $Ru_4(IMes)(CO)_{11}(\mu\text{-}H)_4$, **5** (12% yield), and the dihydride−diruthenium−diplatinum complex $Ru_2Pt_2(IMes)_2(CO)_8(\mu\text{-}H)_2$, **6** (36% yield), at 80 °C. Both compounds **5** and **6** were structurally characterized by single-crystal X-ray diffraction analyses. Compound **5** consists of a Ru_4 tetrahedron with an IMes ligand on Ru1; see Figure 6. There are four hydride ligands that bridge four of the ruthenium bonds. These four hydride ligands (located and refined crystallographically) appear as a broad high-field resonance, at −17.67 ppm, in the ^1H NMR spectrum of the compound. An ORTEP diagram of the molecular structure of compound **5** is shown in Figure 6.

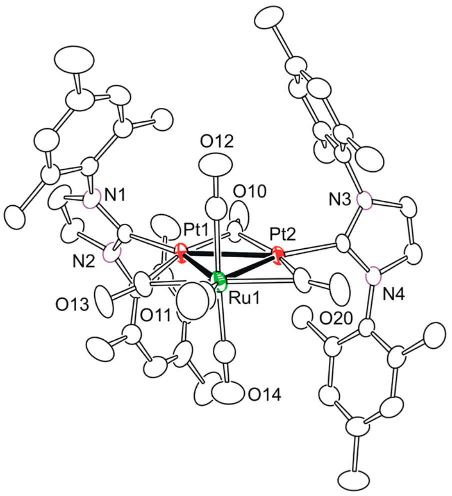

Figure 5. An ORTEP showing the molecular structure of $RuPt_2(IMes)_2(CO)_6$, **4**, at 30% thermal ellipsoid probability. Selected interatomic distances (Å) and angles (deg) are as follows: Pt(1)−Pt(2) = 2.6477(2), Pt(1)−Ru(1) = 2.6898(3), Pt(2)−Ru(1) = 2.7302(3), Pt(2)−Pt(1)−Ru(1) = 61.514(7), Pt(1)−Pt(2)−Ru(1) = 59.997(2), Pt(1)−Ru(1)−Pt(2) = 58.479(8).

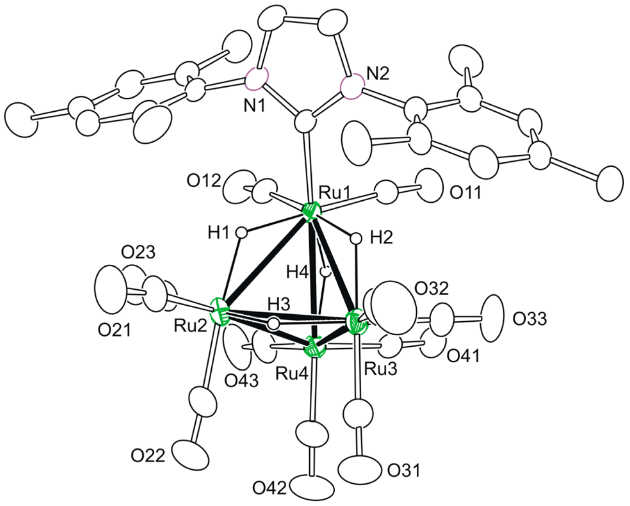

Figure 6. An ORTEP showing the molecular structure of $Ru_4(IMes)(CO)_{11}(\mu\text{-}H)_4$, **5**, at 30% thermal ellipsoid probability. Selected interatomic distances (Å) and angles (deg) are as follows: Ru(1)−Ru(2) = 2.9908(4), Ru(1)−Ru(3) = 3.0154(4), Ru(1)−Ru(4) = 3.0156(3), Ru(2)−Ru(4) = 2.7892(4), Ru(2)−Ru(3) = 2.9348(4), Ru(3)−Ru(4) = 2.7785(4), Ru(2)−Ru(1)−Ru(3) = 58.499(8), Ru(2)−Ru(1)−Ru(4) = 55.337(8), Ru(3)−Ru(1)−Ru(4) = 54.866(9).

This compound is isostructural with $Os_4H_4(CO)_{11}(IMes)$[25] and $Ru_4H_4(CO)_{11}(PPh_3)$.[26] A few years ago, Cooke et al. reported the synthesis of compound **5** by the treatment of $Ru_4(\mu\text{-}H)_4(CO)_{12}$ with Me_3NO and [(IMes)AgCl].[27] After that, Cabeza et al. prepared the same compound using $Ru_4(\mu\text{-}H)_4(CO)_{12}$, potassium *tert*-butoxide, and 1,3-dimesitylimidazolium chloride.[28] Its structure was formulated accurately on the basis of IR, ^1H NMR, mass spectrometry, and elemental analyses. It was also shown that the hydride ligands are fluxional on the NMR time scale, which explains the broad hydride resonance observed at room temperature.[28] We have now obtained a crystal structure for compound **5**, which is shown in Figure 6.

Compound **6** was obtained as a major product from this reaction. As can be seen in Figure 7, the structure of this compound has a butterfly geometry, containing two ruthenium and two platinum atoms. Both of the platinum atoms contain IMes groups, which are present at the “wing-tips” of the butterfly; see Figure 7.

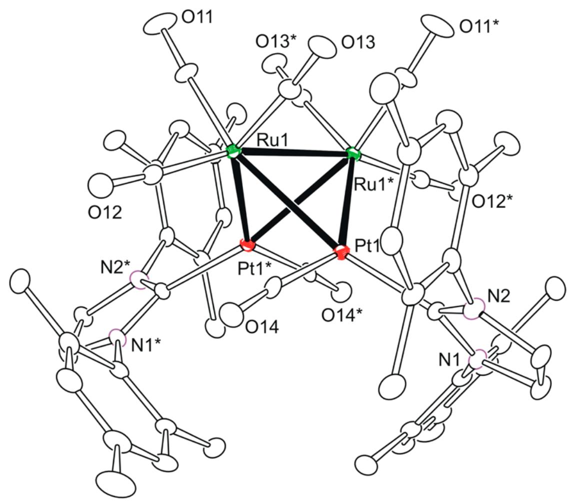

Figure 7. An ORTEP showing the molecular structure of $Ru_2Pt_2(IMes)_2(CO)_8(\mu\text{-}H)_2$, **6**, at 30% thermal ellipsoid probability. Hydride ligands are not shown. Selected interatomic distances (Å) are as follows: Pt(1)−Ru(1) = 2.7136(5), Pt(1)−Ru(1)* = 2.8357(4), Ru(1)−Ru(1)* = 2.7695(8), Ru(1)−Pt(1)* = 2.8356(5).

This dihydride−diruthenium−diplatinum compound contains two ruthenium atoms joined by a Ru−Ru single bond, Ru1−Ru1* = 2.7695(8) Å. Each ruthenium atom is bonded with two Pt(IMes) groups and contains three terminally coordinated carbonyl ligands. The platinum atoms, Pt1 and Pt1*, both have one carbonyl ligand, which is terminally coordinated. There are no bridging carbonyl ligands present in this compound. Appropriately, the complex contains two hydride ligands, which bridge two of the Ru−Pt bonds. The presence of two hydride ligands was not located crystallographically, but they appear as one high-field resonance, in the ^1H NMR spectrum of the compound. These two hydride ligands are equivalent and appear at −9.89 ppm, in the ^1H NMR spectrum of the compound, showing one and two bond coupling to platinum, $^1J_{Pt-H}$ = 560 Hz, $^2J_{Pt-H}$ = 40 Hz. The hydride-bridged Ru−Pt bond lengths, Ru1−Pt1* = 2.8356(5) Å and Ru1*−Pt1 = 2.8357(5) Å, are significantly longer than the unbridged Ru−Pt bond lengths, Ru1−Pt1 = 2.7136(5) Å and Ru1*−Pt1* = 2.7136(5) Å, as expected due to the bond lengthening effects of bridging hydride ligands.[29] Compound **6** is similar in structure to the tetranuclear metal complexes $Pt_2Ru_2(CO)_8(P^tBu_3)_2(\mu\text{-}H)_2$, **7**,[23] $Pt_2Ru_2(CO)_8(PPh_3)_2(\mu\text{-}H)_2$, **8**,[30] and $Pt_2Ru_2(CO)_9(Sn^tBu_3)_2(\mu\text{-}H)_2$, **9**.[31] For complex **6**, the Pt−Pt bond distance is 3.2507(3) Å, which is a long Pt−Pt bond. In complexes **7** and **8**, the Pt−Pt bond distances are 3.1462(5) and 3.137(1) Å, respectively, and can be considered as weak Pt−Pt interactions. In **9** the Pt−Pt distance is short at 2.8105(2) Å. Thus, complex **6** may be interpreted as a butterfly rather than a tetrahedron, with two 16-electron Pt atoms, with a total count of 58 electrons and no Pt−Pt bond.

The formation of compound **6** prompted us to explore the possibility if **6** could eliminate its hydride ligands to yield the unsaturated complex $Ru_2Pt_2(IMes)_2(CO)_8$, **10**. When compound **6** was heated in both benzene and toluene solution, no reaction was observed. Alternatively, compound **10** could be obtained by reaction of **3** with 1 equiv of $Pt(IMes)_2$. However, the reaction of **3** in the presence of 1 equiv of $Pt(IMes)_2$ for an hour gave 38% of compound **4** and 6% of compound **2**. Also, there was no reaction when H_2 was purged through solutions of **4**, both at room temperature and at 80 °C.

CONCLUSION

A goal of this work was to compare the reactivity of the bis-NHC complex $Pt(IMes)_2$ to that reported previously for the bis phosphine complexes $Pt(PR_3)_2$. It has been shown that $Pt(IMes)_2$ just like $Pd(P^tBu_3)_2$ and $Pt(P^tBu_3)_2$ is able to add its Pt(IMes) grouping across Ru−Ru bonds in ruthenium carbonyl cluster complexes. However, the different steric and electronic profile presented by the NHC versus PR_3 ligands has allowed isolation of new and different Ru−Pt−IMes bimetallic cluster compounds, which have been prepared in reasonable yields. One major difference in reactivity is that whereas mononuclear complexes of Ru could not be obtained from the reaction of $Ru(CO)_5$ with $Pd(P^tBu_3)_2$ or $Pt(P^tBu_3)_2$, that picture changed in the successful preparation of complex **4**. In addition, possibly due to increased steric pressure, the bicapped structure presented by $Ru_3Pt_2(IMes)_2(CO)_{12}$ (**2**) differs from analogous reactions of the phosphine-substituted complexes where edge bridging raft-like complexes are formed. The propensity of $Pt(IMes)_2$ to react with ruthenium carbonyl cluster complexes represents a start for the incorporation of Pt−NHC groups into transition metal carbonyl cluster complexes. Additional studies to investigate the differing reactivities, particularly toward small molecule activation, of these and related complexes are in progress.

ASSOCIATED CONTENT

Ⓢ Supporting Information

CIF files for each of the structural analyses. This material is available free of charge via the Internet at http://pubs.acs.org.

AUTHOR INFORMATION

Corresponding Author

*E-mail: captain@miami.edu.

Notes

The authors declare no competing financial interest.

ACKNOWLEDGMENTS

The National Science Foundation (CHE-1300206) is gratefully acknowledged for support of this work as well as for providing funds toward the purchase of an LC−ESI−MS (CHE-0946858).

REFERENCES

(1) Arduengo, A. J., III; Gamper, S. F.; Calabrese, J. C.; Davidson, F. *J. Am. Chem. Soc.* **1994**, *116*, 4391−4394.

(2) (a) Nolan, S. P., Ed. *N-Heterocyclic Carbenes in Synthesis*; Wiley-VCH: Weinheim, Germany, 2006. (b) Glorius, F. *N-Heterocyclic Carbenes in Transition Metal Catalysis*; Springer: Berlin, 2007.

(3) (a) Weskamp, T.; Schattenmann, W. C.; Spiegler, M.; Herrmann, W. A. *Angew. Chem., Int. Ed.* **1998**, *37*, 2490−2493. (b) Huang, J.; Stevens, E. D.; Nolan, S. P.; Petersen, J. L. *J. Am. Chem. Soc.* **1999**, *121*, 2674−2678. (c) Scholl, M.; Ding, S.; Lee, C. W.; Grubbs, R. H. *Org.*

Lett. **1999**, *1*, 953–956. (d) Huang, J.; Stevens, E. D.; Nolan, S. P. *Organometallics* **2000**, *19*, 1194–1197. (e) Choi, T. L.; Grubbs, R. H. *Angew. Chem., Int. Ed.* **2003**, *42*, 1743–1746.

(4) (a) Grasa, G. A.; Viciu, M. S.; Huang, J.; Nolan, S. P. *J. Org. Chem.* **2001**, *66*, 7729–7737. (b) Grasa, G. A.; Viciu, M. S.; Huang, J.; Zhang, C.; Trudell, M. L.; Nolan, S. P. *Organometallics* **2002**, *21*, 2866–2873. (c) Navarro, O.; Kelly, R. A., III; Nolan, S. P. *J. Am. Chem. Soc.* **2003**, *125*, 16194–16195. (d) Marion, N.; Navarro, O.; Mei, J.; Stevens, E. D.; Scott, N. M.; Nolan, S. P. *J. Am. Chem. Soc.* **2006**, *128*, 4101–4111. (e) Navarro, O.; Marion, N.; Mei, J.; Nolan, S. P. *Chem.—Eur. J.* **2006**, *12*, 5142–5148. (f) Lock, J. A.; Albrecht, M.; Peris, E.; Mata, J.; Faller, J. W.; Crabtree, R. H. *Organometallics* **2002**, *21*, 700–706. (g) Peris, E.; Loch, J. A.; Mata, J.; Crabtree, R. H. *Chem. Commun.* **2001**, 201–202.

(5) (a) Hillier, A. C.; Lee, H. M.; Stevens, E. D.; Nolan, S. P. *Organometallics* **2001**, *20*, 4246–4252. (b) Vasquez-Serrano, L. D.; Owens, B. T.; Buriak, J. M. *Chem. Commun.* **2002**, 2518–2519. (c) Sprengers, J. W.; Wassenaar, J.; Clément, N. D.; Cavell, K. J.; Elsevier, C. J. *Angew. Chem., Int. Ed.* **2005**, *44*, 2026–2029. (d) Dharmasena, U. L.; Foucault, H. M.; Dos Santos, E. N.; Fogg, D. E.; Nolan, S. P. *Organometallics* **2005**, *24*, 1056–1058. (e) Albrecht, M.; Crabtree, R. H.; Mata, J.; Peris, E. *Chem. Commun.* **2002**, 32–33. (f) Albrecht, M.; Miecznikowski, J. R.; Samuel, A.; Faller, J. W.; Crabtree, R. H. *Organometallics* **2002**, *21*, 3596–3604.

(6) (a) Lappert, M. F. *J. Organomet. Chem.* **1988**, *358*, 185–214. (b) Herrmann, W. A.; Köcher, C. *Angew. Chem., Int. Ed. Engl.* **1997**, *36*, 2162–2187. (c) Weskamp, T.; Böhm, V. P. W.; Herrmann, W. A. *J. Organomet. Chem.* **2000**, *600*, 12–22. (d) Bourissou, D.; Guerret, O.; Gabbaï, F. P.; Bertrand, G. *Chem. Rev.* **2000**, *100*, 39–91. (e) Herrmann, W. A. *Angew. Chem., Int. Ed.* **2002**, *41*, 1290–1309.

(7) (a) Trnka, T. M.; Grubbs, R. H. *Acc. Chem. Res.* **2001**, *34*, 18–29. (b) Sanford, M. S.; Love, J. A.; Grubbs, R. H. *J. Am. Chem. Soc.* **2001**, *123*, 6543–6554. (c) Huang, J.; Schanz, H. J.; Stevens, E. D.; Nolan, S. P. *Organometallics* **1999**, *18*, 5375–5380.

(8) (a) Markó, I. E.; Stérin, S.; Buisine, O.; Mignani, G.; Branlard, P.; Tinant, B.; Declercq, J. P. *Science* **2002**, *298*, 204–207. (b) Markó, I. E.; Michaud, G.; Berthon-Gelloz, G.; Buisine, O.; Stérin, S. *Adv. Synth. Catal.* **2004**, 1429–1434. (c) Buisine, O.; Berthon-Gelloz, G.; Brière, J. F.; Stérin, S.; Mignani, G.; Branlard, P.; Tinant, B.; Declercq, J. P.; Markó, I. E. *Chem. Commun.* **2005**, 3856–3868.

(9) (a) Duin, M. A.; Clement, N. D.; Cavell, K. J.; Elsevier, C. J. *Chem. Commun.* **2003**, 400–401. (b) Sprengers, J. W.; Mars, M. J.; Duin, M. A.; Cavell, K. J.; Elsevier, C. J. *J. Organomet. Chem.* **2003**, *679*, 149–152.

(10) (a) Toshima, N.; Yonezawa, T. *New J. Chem.* **1998**, 1179–1201. (b) Johnson, B. F. G. *Coord. Chem. Rev.* **1999**, *192*, 1269–1285. (c) Midgley, P. A.; Weyland, M.; Thomas, J. M.; Johnson, B. F. G. *Chem. Commun.* **2001**, 907–908. (d) Nashner, M. S.; Frenkel, A. I.; Somerville, D.; Hills, C. W.; Shapley, J. R.; Nuzzo, R. G. *J. Am. Chem. Soc.* **1998**, *120*, 8093–8101. (e) Nashner, M. S.; Frenkel, A. I.; Adler, D. L.; Shapley, J. R.; Nuzzo, R. G. *J. Am. Chem. Soc.* **1997**, *119*, 7760–7771. (f) Shephard, D. S.; Maschmeyer, T.; Johnson, B. F. G.; Thomas, J. M.; Sankar, G.; Ozkaya, D.; Zhou, W.; Oldroyd, R. D.; Bell, R. G. *Angew. Chem., Int. Ed. Engl.* **1997**, *36*, 2242–2245. (g) Shephard, D. S.; Maschmeyer, T.; Sankar, G.; Thomas, J. M.; Ozkaya, D.; Johnson, B. F. G.; Raja, R.; Oldroyd, R. D.; Bell, R. G. *Chem.—Eur. J.* **1998**, *4*, 1214–1224.

(11) (a) Raja, R.; Sankar, G.; Hermans, S.; Shephard, D. S.; Bromley, S.; Thomas, J. M.; Johnson, B. F. G. *Chem. Commun.* **1999**, 1571–1572. (b) Alexeev, O. S.; Gates, B. C. *Ind. Eng. Chem. Res.* **2003**, *42*, 1571–1587. (c) Goodman, D. W.; Houston, J. E. *Science* **1987**, *236*, 403–409. (d) Ichikawa, M. *Adv. Catal.* **1992**, *38*, 283–400.

(12) (a) Thomas, J. M.; Johnson, B. F. G.; Raja, R.; Sankar, G.; Midgley, P. A. *Acc. Chem. Res.* **2003**, *36*, 20–30. (b) Braunstein, P.; Rose, J. In *Catalysis by Di- and Polynuclear Metal Cluster Complexes*; Adams, R. D., Cotton, F. A., Eds.; VCH: New York, 1998; Chapter 13, p 443.

(13) (a) Raja, R.; Khimyak, T.; Thomas, J. M.; Hermans, S.; Johnson, B. F. G. *Angew. Chem., Int. Ed.* **2001**, *40*, 4638–4642. (b) Hermans, S.; Raja, R.; Thomas, J. M.; Johnson, B. F. G.; Sankar, G.; Gleeson, D. *Angew. Chem., Int. Ed.* **2001**, *40*, 1211–1215. (c) Raja, R.; Sankar, G.; Hermans, S.; Shephard, D. S.; Bromley, S.; Thomas, J. M.; Johnson, B. F. G.; Maschemeyer, T. *Chem. Commun.* **1999**, 1571–1572.

(14) Huq, R.; Poe, A. J.; Chawla, S. *Inorg. Chim. Acta* **1980**, *38*, 121–125.

(15) *Apex2 Version 2.2-0 and SAINT+ Version 7.46A*; Bruker Analytical X-ray System, Inc.: Madison, WI, 2007.

(16) (a) Sheldrick, G. M. *SHELXTL Version 6.1*; Bruker Analytical X-ray Systems, Inc.: Madison, WI, 2000. (b) Sheldrick, G. M. *Acta Crystallogr.* **2008**, *A64*, 112–122.

(17) Cabeza, J. A.; del Rio, I.; Miguel, D.; Perez-Carreno, E.; Sanchez-Vega, M. G. *Organometallics* **2008**, *27*, 211–217.

(18) Adams, R. D.; Captain, B.; Zhu, L. *J. Am. Chem. Soc.* **2007**, *129*, 2454–2455.

(19) (a) Adams, R. D.; Captain, B.; Fu, W.; Smith, M. D. *J. Am. Chem. Soc.* **2002**, *124*, 5628–5629. (b) Adams, R. D.; Captain, B.; Fu, W.; Hall, M. B.; Manson, J.; Smith, M. D.; Webster, C. E. *J. Am. Chem. Soc.* **2004**, *126*, 5253–5267.

(20) Adams, R. D.; Captain, B.; Fu, W.; Smith, M. D.; Zhu, L. *J. Cluster Sci.* **2006**, *17*, 87–95.

(21) Adams, R. D.; Captain, B.; Zhu, L. *Inorg. Chem.* **2006**, *45*, 430–436.

(22) Moss, J. R.; Graham, W. A. G. *J. Chem. Soc., Dalton Trans.* **1977**, 95–99.

(23) Adams, R. D.; Captain, B.; Fu, W.; Hall, M. B.; Smith, M. D.; Webster, C. E. *Inorg. Chem.* **2004**, *43*, 3921–3929.

(24) Adams, R. D.; Captain, B. *Acc. Chem. Res.* **2009**, *42*, 409–418.

(25) Cooke, C. E.; Jennings, M. C.; Pomeroy, R. K.; Clyburne, J. A. C. *Organometallics* **2007**, *26*, 6059–6062.

(26) Haerkoenen, A. U.; Ahlgren, M.; Pakkanen, T. A.; Pursiainen, J. *J. Organomet. Chem.* **1997**, *530*, 191–197.

(27) Cooke, C. E.; Jennings, M. C.; Katz, M. J.; Pomeroy, R. K.; Clyburne, J. A. C. *Organometallics* **2008**, *27*, 5777–5799.

(28) Cabeza, J. A.; del Río, I.; Fernández-Colinas, J. M.; Pérez-Carreño, E.; Sánchez-Vega, M. G.; Vázquez-García, D. *Organometallics* **2009**, *28*, 1832–1837.

(29) Teller, R. G.; Bau, R. *Struct. Bonding (Berlin)* **1981**, *41*, 1.

(30) Adams, R. D.; Bunz, U.; Captain, B.; Fu, W.; Steffen, W. *J. Organomet. Chem.* **2000**, *614*, 75–82.

(31) Manzoli, M.; Shetti, V. N.; Blaine, J. A. L.; Zhu, L.; Isrow, D.; Yempally, V.; Captain, B.; Coluccia, S.; Raja, R.; Gianotti, E. *Daltan Trans.* **2012**, *41*, 982–989.